Transition moments and excited-state first-order properties in the coupled-cluster model CC2 using the resolution-of-the-identity approximation

Christof Hättig
Forschungszentrum Karlsruhe, Institute of Nanotechnology, P.O. Box 3640, D-76021 Karlsruhe, Germany

Andreas Köhn
Universität Karlsruhe (TH), Institut für Physikalische Chemie, Lehrstuhl für Theoretische Chemie, Kaiserstraße 12, D-76128 Karlsruhe, Germany

(Received 19 June 2002; accepted 23 July 2002)

An implementation of transition moments and excited-state first-order properties is reported for the approximate coupled-cluster singles-and-doubles model (CC2) using the resolution of the identity (RI) approximation. In parallel to the previously reported code for the ground- and excited-state amplitude equations, we utilize a partitioned form of the CC2 equations and thus eliminate the need to store any N^4 intermediates. This opens the perspective for applications on molecules with 30 and more atoms. The accuracy of the RI approximation is tested for a set of 29 molecules for the aug-cc-pVXZ ($X=D,T,Q$) basis sets in connection with the recently optimized auxiliary basis sets. These auxiliary basis sets are found to be sufficient even for the description of diffuse states. The RI error is compared to the usual basis set error and is demonstrated to be insignificant. © *2002 American Institute of Physics.* [DOI: 10.1063/1.1506918]

I. INTRODUCTION

Transition moments and excited-state first-order properties are important links between quantum-chemical calculations and experimental observations, which allow a better characterization of excited states than just the excitation energies. Transition moments are directly related, e.g., to absorption and emission strengths, rotation strengths, or excited-state lifetimes. First-order properties give valuable information about the character of the excited state, for instance whether valence or Rydberg states are present or whether charge transfer takes place in the excitation process. Response theory[1–5] has shown to provide a theoretically very clear-cut and well-defined access to these properties. It has been successfully applied to variational wave functions [Hartree–Fock (HF), density functional theory (DFT), multiconfiguration self-consistent field (MCSCF), and configuration interaction (CI)] (Refs. 4 and 6–8) and nonvariational wave functions, such as the coupled-cluster (CC) models (Refs. 9–12).

The great advantage of the coupled-cluster approach is that it gives a systematic hierarchy of well-defined blackbox methods with increasing accuracy,[13,14] named CCS, CC2, CCSD, CC3,[15–17] etc., for which response-theory-based codes for excited states and their properties have been implemented. Among these, CC2 is the computationally cheapest method that incorporates dynamical correlation. The quality of the description of the ground state is comparable to MP2, but CC2 is better suited for response theory.[15]

The applicability of CC2 can be largely extended by employing a partitioned form of the CC2 equations,[18] which avoids the storage of intermediates scaling as N^4, either on a disk or in memory. The necessary recalculation of the T_2 amplitudes can be accomplished very efficiently employing the resolution-of-the-identity (RI) approximation.[19,20] Using this T_2-direct methodology, calculations with more than 1000 basis functions in C_1 symmetry have been shown to be feasible.[18]

In the present communication, we present an analogous partitioned, T_2-direct formulation of the response equations, which need to be solved to obtain transition moments and excited-state first-order properties (Sec. II), and give a brief description of the implementation and how the RI approximation is exploited (Sec. III). As pointed out above, these quantities provide itself important information about the vertical transitions and the excited states. The implementation of this functionality is also the first step for the development of analytic gradients for excited states, since these require the solution of the same response equations and similar one-electron densities. Analytic RI-CC2 gradients for excited states will open the perspective of accurate correlated *ab initio* geometry optimizations for excited states of molecules with 30 or more atoms.

The error introduced by the RI approximation has been shown to be very small for selected examples.[18] Detailed studies have been carried out for the RI-MP2 (Ref. 20) ground-state correlation energies.[21,22] In one of the latter studies,[22] it was established that the conventional basis set truncation error is between one and two orders of magnitude larger than the corresponding error introduced by the RI approximation (RI error). In Sec. IV we will present a similar study for excited states obtained from the CC2 method, using the augmented correlation consistent basis sets aug-cc-pVXZ ($X=D,T,Q$) and the corresponding auxiliary basis sets. The size of the RI error is evaluated for excitation energies, oscillator strengths, dipole moments, and the sec-

 © 2002 American Institute of Physics

Downloaded 02 Oct 2002 to 141.52.232.84. Redistribution subject to AIP license or copyright, see http://ojps.aip.org/jcpo/jcpcr.jsp

ond moments of the difference density. For selected states, we will also examine the conventional basis set error, which is to our knowledge the first study of that kind. A short account of the efficiency is given in Sec. V.

II. THEORY

The CC2 model was defined by Christiansen *et al.*[15] using a Møller–Plesset-type partitioning of the Hamiltonian

$$H=F+U, \tag{1}$$

where F is the Fock matrix and U the fluctuation potential. Retaining only those terms in the double-excitation part of the cluster equations—also known as the vector function—which enter up to first order in U leads to the following equations for the cluster operators $T_i=\Sigma_{\mu_i} t_{\mu_i}\tau_{\mu_i}$ with $i=1,2$:

$$\Omega_{\mu_1}=\langle\mu_1|\hat{H}+[\hat{H},T_2]|\mathrm{HF}\rangle=0, \tag{2}$$

$$\Omega_{\mu_2}=\langle\mu_2|\hat{H}+[F,T_2]|\mathrm{HF}\rangle=0. \tag{3}$$

Here, $|\mathrm{HF}\rangle$ is the closed-shell Hartree–Fock ground-state determinant and $\{\langle\mu_1|,\langle\mu_2|\}$ represent the (singlet) singles and doubles projection manifold. $\hat{H}$ is the T_1-transformed Hamiltonian[23]

$$\hat{H}=e^{-T_1}He^{T_1}. \tag{4}$$

The double-excitation part of the cluster equations, Ω_{μ_2}, can be inverted directly, recovering an MP2-like expression for the doubles amplitudes,

$$t_{ij}^{ab}=\frac{1}{1+\delta_{ij}\delta_{ab}}\frac{(ai\hat{|}bj)}{\epsilon_i-\epsilon_a+\epsilon_j-\epsilon_b}, \tag{5}$$

with T_1-transformed two-electron integrals

$$(pq\hat{|}rs)=\sum_{\mu\nu\kappa\lambda}\Lambda^p_{\mu p}\Lambda^h_{\nu q}\Lambda^p_{\kappa r}\Lambda^h_{\lambda s}(\mu\nu|\kappa\lambda), \tag{6}$$

$$\Lambda^p=\mathbf{C}(\mathbf{1}-\mathbf{t}_1^T),\quad \Lambda^h=\mathbf{C}(\mathbf{1}+\mathbf{t}_1). \tag{7}$$

Here and in the following, indices i, j, k, etc., denote occupied molecular orbitals (MO's), a, b, c, etc., virtual MO's, and p, q, r, s general (occupied or virtual) MO's, while Greek indices μ, ν, κ, etc., indicate basis functions. $\mathbf{C}$ is the usual transformation matrix for canonical MO's. Carets are used to indicate that the quantities refer to the similarity transformed Λ^p, Λ^h basis. Inserting Eq. (5) into Eq. (2), one obtains an effective equation for only the singles amplitudes. This allows us to avoid the storage of the doubles amplitudes and to recalculate these whenever needed via Eq. (5). By virtue of the RI approximation this can be done very efficiently, as demonstrated in a previous communication.[18] The four-index electron repulsion integrals (ERI's) in the atomic orbital basis are expanded in an auxiliary basis $\{P\}$ as

$$(\mu\nu|\kappa\lambda)=\sum_{PQ}(\mu\nu|P)V^{-1}_{PQ}(Q|\kappa\lambda), \tag{8}$$

where $(\mu\nu|P)$ are three-index ERI's and the Coulomb metric[19]

$$V_{PQ}=(P|Q) \tag{9}$$

is constituted by two-index ERI's. It is convenient to use a symmetric decomposition of the metric V_{PQ} and to introduce the quantity

$$\hat{B}^Q_{pq}=\sum_\mu \Lambda^p_{\mu p}\sum_\nu \Lambda^h_{\nu q}\sum_P (\mu\nu|P)V^{-1/2}_{PQ}. \tag{10}$$

The transformation into the MO basis scales now merely as ON_xN^2, where O is the number of occupied orbitals, N the number of one-electron basis functions, and N_x the number of auxiliary basis functions. The disk space required for storage of $\hat{B}^Q_{ai}$ is about OVN_x words, V being the number of virtual orbitals. The formation of four-index MO integrals

$$(ai\hat{|}bj)=\sum_Q \hat{B}^Q_{ai}\hat{B}^Q_{bj} \tag{11}$$

is still scaling with the fifth power of the system size, however, with a small prefactor since two indices run only over occupied orbitals. For a detailed algorithm for the ground-state vector function see Ref. 18.

The CC2 excitation energies are obtained as the eigenvalues of the unsymmetric Jacobian matrix

$$\mathbf{A}_{\mu_i\nu_j}=\frac{\partial\Omega_{\mu_i}}{\partial t_{\nu_j}}. \tag{12}$$

The doubles–doubles block $\mathbf{A}_{\mu_2\nu_2}=\delta_{\mu_2\nu_2}\epsilon_{\mu_2}$ is diagonal with diagonal elements equal to the SCF orbital energy differences $\epsilon_{aibj}=\epsilon_a-\epsilon_i+\epsilon_b-\epsilon_j$. This enables us to define an effective Jacobian matrix for the singles–singles block,

$$\mathbf{A}^{\mathrm{eff}}_{\mu_1\nu_1}(\omega)=\mathbf{A}_{\mu_1\nu_1}-\sum_{\gamma_2}\frac{\mathbf{A}_{\mu_1\gamma_2}\mathbf{A}_{\gamma_2\nu_1}}{\epsilon_{\gamma_2}-\omega}, \tag{13}$$

which reduces the dimensionality of the eigenvalue problem and again avoids storage of the doubles part of the trial vectors. However, the effective eigenvalue problem is no longer linear since $\mathbf{A}^{\mathrm{eff}}(\omega)$ depends on the eigenvalue ω. In Ref. 18 a combination of a semilinear eigenvalue solver and a DIIS algorithm has been developed for the iterative solution of the right-hand-side eigenvalue problem,

$$\sum_{\nu_1}\mathbf{A}^{\mathrm{eff}}_{\mu_1\nu_1}(\omega)E_{\nu_1}(\omega)=\omega E_{\mu_1}(\omega), \tag{14}$$

which in practice typically requires the same number of iterations as a conventional algorithm would need for the linear eigenvalue problem. In the same reference, explicit expressions were given for the transformation of a trial vector R_{μ_1} with the effective Jacobian where the trial vector appears on the right-hand side:

$$\sigma_{\mu_1}(\omega,R_1)=\sum_{\nu_1}\mathbf{A}^{\mathrm{eff}}_{\mu_1\nu_1}(\omega)R_{\nu_1}(\omega). \tag{15}$$

For the calculation of transition moments and properties the left eigenvectors $\overline{E}_{\mu_1}(-\omega)$ are needed as well. The transformation of a trial vector with the effective Jacobian from the left,

Downloaded 02 Oct 2002 to 141.52.232.84. Redistribution subject to AIP license or copyright, see http://ojps.aip.org/jcpo/jcpcr.jsp

TABLE I. Explicit expressions for vectors transformed with the effective Jacobian either from the left or from the right and for effective right-hand-side vectors derived from $L\mathbf{B}R$-like contractions. All three types of vectors can be split into six contributions, $\sigma_S=\sigma_S^0+\sigma_S^G+\sigma_S^H+\sigma_S^I+\sigma_S^J$, which involve the same contractions for all vectors.

σ_S	$\mathbf{A}_{SS}^{(\mathrm{eff})}(\omega_R)R_S$	$L_S\mathbf{A}_{SS}^{(\mathrm{eff})}(\omega_L)$	$(L\mathbf{B}R)_S-\Sigma_D\frac{(L\mathbf{B}R)_D\mathbf{A}_{DS}}{\epsilon_D+\omega_L-\omega_R}$
σ_{ai}^0	$\Sigma_d E_{ad}R_{di}-\Sigma_l R_{al}E_{li}$	$\Sigma_d E_{da}L_{di}-\Sigma_l L_{al}E_{il}$	$\Sigma_d\overline{E}_{da}L_{di}-\Sigma_l L_{al}\overline{E}_{il}$
σ_{ai}^G	$\Sigma_{dlc}[2R_{il}^{cd}-R_{il}^{dc}](ld\hat{\vert}ac)$	$\Sigma_{dlc}L_{il}^{cd}(ld\hat{\vert}ca)$	$\Sigma_{dlc}F_{il}^{cd}(ld\hat{\vert}ca)+\Sigma_{dlc}L_{il}^{cd}(dl\bar{\vert}ca)$
σ_{ai}^H	$-\Sigma_{dlk}[2R_{kl}^{ad}-R_{kl}^{da}](ld\hat{\vert}ki)$	$-\Sigma_{dlk}L_{kl}^{ad}(ld\hat{\vert}ik)$	$-\Sigma_{dlk}F_{kl}^{ad}(ld\hat{\vert}ik)-\Sigma_{dlk}L_{kl}^{ad}(dl\bar{\vert}ik)$
σ_{ai}^I	$\Sigma_{ck}([2R_{ik}^{ac}-R_{ik}^{ca}]\hat{F}_{kc}+[2t_{ik}^{ac}-t_{ki}^{ac}]\overline{F}_{kc})$	$\Sigma_{ck}[2(kc\vert ia)-(ic\vert ka)]C_{ck}$	$\Sigma_{ck}[2(kc\vert ia)-(ic\vert ka)]\overline{C}_{ck}$
σ_{ai}^J	$\Sigma_{ck}[2(kc\vert ai)-(ki\vert ac)]R_{ck}$	$\Sigma_{ck}L_{ck}[2(ck\vert ia)-(ca\hat{\vert}ik)]$	$\Sigma_{ck}L_{ck}[2(ck\vert\bar{ia})-(ca\vert ik)]$
	$\overline{F}_{ck}=\Sigma_{dl}[2(kc\vert ld)-(kd\vert lc)]R_{dl}$	$C_{ck}=\Sigma_{dl}[2t_{kl}^{cd}-t_{kl}^{dc}]L_{dl}$	$\overline{C}_{ck}=\Sigma_{dl}[2R_{kl}^{cd}-R_{kl}^{dc}]L_{dl}$
	$E_{ab}=\hat{F}_{ab}-\Sigma_{dkl}(2t_{kl}^{ad}-t_{lk}^{ad})(ld\vert kb)$		$\overline{E}_{ab}=\overline{F}_{ab}-\Sigma_{dkl}(2R_{kl}^{ad}-R_{kl}^{da})(ld\vert kb)$
	$E_{ji}=\hat{F}_{ji}+\Sigma_{cdk}(2t_{ik}^{cd}-t_{ki}^{cd})(kd\vert jc)$		$\overline{E}_{ji}=\overline{F}_{ji}+\Sigma_{cdk}(2R_{ik}^{cd}-R_{ik}^{dc})(kd\vert jc)$

$$\overline{\sigma}_{\nu_1}(-\omega,L_1)=\sum_{\mu_1}L_{\mu_1}(-\omega)\mathbf{A}_{\mu_1\nu_1}^{\mathrm{eff}}(\omega), \tag{16}$$

can be formulated in a similar way. Again, the doubles part of the trial vector need not be stored on disk, but can instead be calculated on-the-fly as

$$L_{ij}^{ab}(-\omega)=\frac{2(ia\breve{\vert}jb)-(ib\breve{\vert}ja)+P_{ij}^{ab}[2L_{ai}\hat{F}_{jb}-L_{bi}\hat{F}_{ja}]}{\epsilon_i-\epsilon_a+\epsilon_j-\epsilon_b+\omega}, \tag{17}$$

where $\hat{F}$ denotes the T_1-transformed Fock matrix,[23]

$$\hat{F}_{pq}=\sum_{pq}\Lambda_{\mu p}^p\Lambda_{\nu q}^h F_{\mu\nu}+\sum_{ck}[2(pq\hat{\vert}ck)-(pk\hat{\vert}cq)]t_{ck},$$

and P_{ij}^{ab} is an operator which symmetrizes the index pairs ia, jb as $P_{ij}^{ab}t_{ij}^{ab}=t_{ij}^{ab}+t_{ji}^{ba}$. The modified two-electron MO integrals

$$(pq\breve{\vert}rs)=P_{pr}^{qs}\sum_{\mu\nu\kappa\lambda}(\breve{\Lambda}_{\mu p}^p\Lambda_{\nu q}^h+\Lambda_{\mu p}^p\breve{\Lambda}_{\nu q}^h)\Lambda_{\kappa r}^p\Lambda_{\lambda s}^h(\mu\nu\vert\kappa\lambda) \tag{18}$$

can be calculated using a similar algorithm as in Ref. 18 with $\breve{\Lambda}^p=\Lambda^pL_1$ and $\breve{\Lambda}^h=-\Lambda^hL_1^T$. Explicit expressions for $\overline{\sigma}(-\omega,L_1)$ can be found in Table I. The left eigenvectors of $\mathbf{A}^{\mathrm{eff}}$ can then be obtained iteratively. Taking right eigenvectors as start vectors, the DIIS algorithm proposed in Ref. 18 proves to be very stable and converges fast.

For CC methods the expressions for ground-state first- and higher-order properties and for transition moments are most conveniently derived using the Lagrangian[24]

$$L=E_{\mathrm{CC}}+\sum_i\sum_{\mu_i}\overline{t}_{\mu_i}\Omega_{\mu_i}, \tag{19}$$

where $E_{\mathrm{CC}}=\langle\mathrm{HF}\vert\hat{H}+[\hat{H},T_2]\vert\mathrm{HF}\rangle$ is the ground-state energy. The Lagrangian multipliers $\overline{t}$ are obtained as a solution of the linear equations

$$\overline{t}\mathbf{A}=-\eta^{(0)}, \tag{20}$$

$$\eta_\mu^{(0)}=\frac{\partial E_{\mathrm{CC}}}{\partial t_\mu}. \tag{21}$$

From the cluster amplitudes t_μ and the Lagrangian multipliers $\overline{t}_\mu$ the unrelaxed ground-state one-particle density matrix in the Λ^p, Λ^h basis, D_{pq}^Λ, can be calculated by the expression given in Table II.

Transition moments are obtained from the residues of the linear response function. Due to the nonvariational structure of CC response theory, one obtains for the one-photon transition strength[25]

$$S_{V_1V_2}^{0f}=\frac{1}{2}\{M_{0\leftarrow f}^{V_1}M_{f\leftarrow 0}^{V_2}+(M_{0\leftarrow f}^{V_2}M_{f\leftarrow 0}^{V_1})^*\}, \tag{22}$$

where the "left" ($M_{0\leftarrow f}^V$) and "right" ($M_{f\leftarrow 0}^V$) transition moments can be calculated as

$$M_{0\leftarrow f}^V=\sum_{pq}[D_{pq}^\eta(E)+D_{pq}^\xi(\overline{M})]\hat{V}_{pq}, \tag{23}$$

$$M_{f\leftarrow 0}^V=\sum_{pq}D_{pq}^\xi(\overline{E})\hat{V}_{pq}. \tag{24}$$

TABLE II. Expressions for the one-particle density matrices D^Λ, $D^\xi(L)$, and $D^A(L,R)$. The density matrix $D^\eta(R)$ can be expressed as $D^\eta=D^{\eta,0}+D^A(\overline{t},R)$, where $D_{ia}^{\eta,0}=2R_{ia}$.

Block	D^Λ	$D^\xi(L)$	$D^A(L,R)$
occ/occ: $D_{ij}=$	$2\delta_{ij}-\Sigma_{abk}\overline{t}_{jk}^{ab}t_{ik}^{ab}$	$-\Sigma_{abk}L_{jk}^{ab}t_{ik}^{ab}$	$-\Sigma_aL_{aj}R_{ai}-\Sigma_{abk}L_{jk}^{ab}R_{ik}^{ab}$
occ/vir: $D_{ia}=$	$\Sigma_{ck}\overline{t}_{ck}[2t_{ik}^{ac}-t_{ki}^{ac}]$	$\Sigma_{ck}L_{ck}[2t_{ik}^{ac}-t_{ki}^{ac}]$	$\Sigma_{ck}L_{ck}R_{ik}^{ac}$
			$-\Sigma_b(\Sigma_{kjc}L_{kj}^{bc}t_{kj}^{ac})R_{bi}$
			$-\Sigma_j(\Sigma_{cbk}L_{jk}^{cb}t_{ik}^{cb})R_{aj}$
vir/occ: $D_{ai}=$	$\overline{t}_{ai}$	L_{ai}	0
vir/vir: $D_{ab}=$	$\Sigma_{ijc}\overline{t}_{ij}^{ac}t_{ij}^{bc}$	$\Sigma_{ijc}L_{ij}^{ac}t_{ij}^{bc}$	$\Sigma_iL_{ai}R_{bi}+\Sigma_{ijc}L_{ij}^{ac}R_{ij}^{bc}$

Downloaded 02 Oct 2002 to 141.52.232.84. Redistribution subject to AIP license or copyright, see http://ojps.aip.org/jcpo/jcpcr.jsp

In the latter equations we introduced the generalized one-particle (transition) density matrices $D^{\eta}(R)$ and $D^{\xi}(L)$ and the transition moment Lagrangian multipliers[24] $\overline{M}$. Explicit expressions for $D^{\eta}(R)$ and $D^{\xi}(L)$ are given in Table II. The Lagrangian multipliers $\overline{M}$ are obtained as a solution of the linear equations

$$\overline{M}(\omega)(\mathbf{A}+\omega\mathbf{1})=-\overline{m}(\omega)=-\mathbf{F}E(\omega), \tag{25}$$

where the matrix $\mathbf{F}$ is defined as partial second derivative of the Lagrangian Eq. (19):

$$F_{\mu\nu}=\frac{\partial^2 L}{\partial t_\mu \partial t_\nu}. \tag{26}$$

The difference between the unrelaxed one-particle densities of the ground state and an excited state is obtained as

$$D^{ex,diff}_{pq}=D^{A}_{pq}(\overline{E},E)+D^{\xi}_{pq}(\overline{N}). \tag{27}$$

Explicit expressions for the generalized one-particle density matrices $D^{A}(L,R)$ and $D^{\xi}(L)$ in the Λ^p, Λ^h basis are given in Table II. In Eq. (27) we introduced the excited-state Lagrangian multipliers,[24] $\overline{N}$ defined by the linear equation

$$\overline{N}\mathbf{A}=-\overline{n}=-\overline{E}(-\omega)\mathbf{B}E(\omega), \tag{28}$$

with

$$\mathbf{B}_{\mu\nu\gamma}=\frac{\partial \mathbf{A}_{\mu\nu}}{\partial t_\gamma}. \tag{29}$$

The additional sets of linear equations that need to be solved for the Lagrangian multipliers $\overline{t}$, $\overline{M}$, and $\overline{N}$ have the common form

$$L(\omega)(\mathbf{A}+\omega\mathbf{1})=-\overline{\xi}(\omega). \tag{30}$$

Exploiting the structure of the CC2 Jacobian, Eq. (30), can for the single-excitation part be cast into the partitioned form

$$L_{\mu_1}(\omega)[\mathbf{A}^{\mathrm{eff}}_{\mu_1\nu_1}(-\omega)+\omega\mathbf{1}]=-\overline{\xi}^{\mathrm{eff}}_{\nu_1}(\omega), \tag{31}$$

$$\overline{\xi}^{\mathrm{eff}}_{\nu_1}(\omega)=\overline{\xi}_{\nu_1}(\omega)-\sum_{\gamma_2}\frac{\overline{\xi}_{\gamma_2}\mathbf{A}_{\gamma_2\nu_1}}{\epsilon_{\gamma_2}+\omega}. \tag{32}$$

Unlike for the eigenvalue problem, no nonlinearity is introduced by this reformulation; thus for the solution of Eq. (31) the standard algorithms can be applied. Again, storage of the doubles parts of the right-hand-side vector and the Lagrangian multipliers is no longer required. Whenever needed, the double-excitation part of the solution vector can be calculated on-the-fly as

$$L_{\mu_2}(\omega)=-\frac{\overline{\xi}_{\mu_2}(\omega)+\Sigma_{\nu_1}L_{\nu_1}(\omega)\mathbf{A}_{\nu_1\mu_2}}{\epsilon_{\mu_2}+\omega}. \tag{33}$$

The effective right-hand-side vector for the ground-state Lagrangian multipliers $\overline{t}$ is obtained as

$$\eta^{\mathrm{eff}}_{ia}=2\hat{F}_{ia}+\sum_{cdk}\tilde{\eta}^{cd}_{ki}(ck\lceil da)+\sum_{ckl}\tilde{\eta}^{ca}_{kl}(ck\lceil il), \tag{34}$$

with

$$\tilde{\eta}^{ab}_{ij}=-2\frac{2(ia|jb)-(ib|ja)}{\epsilon_a-\epsilon_i+\epsilon_b-\epsilon_j}. \tag{35}$$

The doubles part $\overline{t}^{ab}_{ij}$ can be calculated from

$$\overline{t}^{ab}_{ij}=\tilde{\eta}^{ab}_{ij}+\frac{2(ia\breve{|}jb)-(ib\breve{|}ja)+P^{ab}_{ij}[2\overline{t}_{ai}\hat{F}_{jb}-\overline{t}_{bi}\hat{F}_{ja}]}{\epsilon_i-\epsilon_a+\epsilon_j-\epsilon_b}. \tag{36}$$

The transformed two-electron integrals $(ia\breve{|}jb)$ are obtained as in Eq. (18), but with transformation matrices $\breve{\Lambda}^p=\Lambda^p\overline{t}_{\mu_1}$ and $\breve{\Lambda}^h=-\Lambda^h\overline{t}^{T}_{\mu_1}$. Similarly, the effective right-hand side for the transition moment Lagrangian multipliers $\overline{M}$ is obtained as

$$\overline{m}^{\mathrm{eff}}_{\mu_1}(\omega)=\sum_{\nu_1}\mathbf{F}_{\nu_1\mu_1}E_{\nu_1}(\omega)+\sum_{\nu_2}\mathbf{F}_{\nu_2\mu_1}E_{\nu_2}(\omega)-\sum_{\nu_2}\frac{\overline{m}_{\nu_2}(\omega)\mathbf{A}_{\nu_2\mu 1}}{\epsilon_{\nu_2}+\omega}, \tag{37}$$

whereas the effective right-hand side for the excited-state Lagrangian multipliers $\overline{N}$ is

$$\overline{n}^{\mathrm{eff}}_{\mu_1}=\sum_{i=1}^{2}\sum_{\gamma_i\nu_1}\overline{E}_{\gamma_i}(-\omega)\mathbf{B}_{\gamma_i\nu_1\mu_1}E_{\nu_1}(\omega)+\sum_{\gamma_1\nu_2}\overline{E}_{\gamma_1}(-\omega)\mathbf{B}_{\gamma_1\nu_2\mu_1}E_{\nu_2}(\omega)-\sum_{\nu_2}\frac{\overline{n}_{\nu_2}\mathbf{A}_{\nu_2\mu 1}}{\epsilon_{\nu_2}}. \tag{38}$$

The matrices $\mathbf{F}$ and $\mathbf{B}$ are related by the equation

$$\mathbf{F}_{\mu\nu}=\frac{\partial \eta^{(0)}_{\mu}}{\partial t_\nu}+\sum_{\gamma}\overline{t}_{\gamma}\mathbf{B}_{\gamma\mu\nu}, \tag{39}$$

where the first term gives a nonvanishing contribution only for the singles–singles block:

$$\frac{\partial \eta^{(0)}_{\mu_1}}{\partial t_{\nu_1}}=\langle \mathrm{HF}|[[H,\tau_{\mu_1}],\tau_{\nu_1}]|\mathrm{HF}\rangle=\mathbf{F}^{(0)}_{\mu_1\nu_1}. \tag{40}$$

Using this relation Eq. (37) can be cast into almost the same form as Eq. (38):

$$\overline{m}^{\mathrm{eff}}_{\mu_1}(\omega)=\sum_{\nu_1}\mathbf{F}^{(0)}_{\nu_1\mu_1}E_{\nu_1}(\omega)+\sum_{i=1}^{2}\sum_{\gamma_i\nu_1}\overline{t}_{\gamma_i}\mathbf{B}_{\gamma_i\nu_1\mu_1}E_{\nu_1}(\omega)+\sum_{\gamma_1\nu_2}\overline{t}_{\gamma_1}\mathbf{B}_{\gamma_1\nu_2\mu_1}E_{\nu_2}(\omega)-\sum_{\nu_2}\frac{\overline{m}_{\nu_2}(\omega)\mathbf{A}_{\nu_2\mu 1}}{\epsilon_{\nu_2}+\omega}. \tag{41}$$

The double-excitation parts of the right-hand-side vectors $\overline{m}_{\mu_2}$ and $\overline{n}_{\mu_2}$ are

Downloaded 02 Oct 2002 to 141.52.232.84. Redistribution subject to AIP license or copyright, see http://ojps.aip.org/jcpo/jcpcr.jsp

$$\bar{m}_{\mu_2}(\omega)=\sum_{\nu_1\gamma_2}\bar{t}_{\nu_1}\mathbf{B}_{\nu_1\gamma_1\mu_2}E_{\gamma_1}(\omega), \tag{42}$$

$$\bar{n}_{\mu_2}=\sum_{\nu_1\gamma_2}\bar{E}_{\nu_1}(-\omega)\mathbf{B}_{\nu_1\gamma_1\mu_2}E_{\gamma_1}(\omega). \tag{43}$$

The effective right-hand-side vector $\bar{m}^{\text{eff}}$ can thus be obtained from the same routines as $\bar{n}^{\text{eff}}$ by replacing $\bar{E}(-\omega)$ with $\bar{t}$. The expression for the only remaining contribution is

$$\sum_{bj}\mathbf{F}^{(0)}_{bj,ai}E_{bj}(\omega)=\sum_{bj}[2(ia|jb)-(ib|ja)]E_{bj}(\omega). \tag{44}$$

From Table I it is apparent that the necessary contractions for the calculation of $\bar{m}^{\text{eff}}$ and $\bar{n}^{\text{eff}}$, which are given in the last column, resemble those of the Jacobian right and left transformations. The double-excitation amplitudes $F^{ab}_{ij}=(L\mathbf{B}R)_{aibj}$ are

$$F^{ab}_{ij}=\frac{2\widetilde{(ai|bj)}-\widetilde{(aj|bi)}+P^{ab}_{ij}(2L_{ai}\bar{F}_{bj}-L_{aj}\bar{F}_{bi})}{\epsilon_i-\epsilon_a+\epsilon_j-\epsilon_b}, \tag{45}$$

with the one-index transformed integrals

$$\widetilde{(ai|bj)}=-P^{ab}_{ij}\Big(\sum_{kc}L_{ci}R_{ck}(ka\hat{|}bj)+\sum_{ck}L_{ak}R_{ck}(ic\hat{|}bj)\Big). \tag{46}$$

The integrals $(pq|\bar{rs})$ needed for some contributions in the last column of Table I are defined as

$$(pq|\bar{rs})=P^{pr}_{qs}\sum_{\mu\nu\kappa\lambda}(\bar{\Lambda}^p_{\mu p}\Lambda^h_{\nu q}+\Lambda^p_{\mu p}\bar{\Lambda}^h_{\nu q})\times\Lambda^p_{\kappa r}\Lambda^h_{\lambda s}(\mu\nu|\kappa\lambda),$$

with $\bar{\Lambda}^p=-\mathbf{C}R_1^T$ and $\bar{\Lambda}^h=\mathbf{C}R_1$, and the response Fock matrix $\bar{F}_{pq}$ is defined as

$$\bar{F}_{pq}=\sum_{pq}(\bar{\Lambda}^p_{\mu p}\Lambda^h_{\nu q}+\Lambda^p_{\mu p}\bar{\Lambda}^h_{\nu q})F_{\mu\nu}+\sum_{ck}[2(pq\hat{|}ck)-(pk\hat{|}cq)]R_{ck}.$$

A generalization of the above approach for excited triplet states was reported in Refs. 26 and 27.

III. IMPLEMENTATION

The calculation of transition moments and excited-state first-order properties within the RI-CC2 approach follows a similar route as used in conventional CC2 implementations:

(i) After solution of the ground-state cluster equations, the excitation energies and the single-excitation parts of the eigenvectors are determined by solving the effective eigenvalue problem, Eq. (14), and the corresponding equation of the left eigenvectors.

(ii) Then the effective right-hand-side vector η^{eff} is calculated via Eq. (34) and the equations for ground-state Lagrangian multipliers, Eq. (20), are solved.

(iii) After the ground-state Lagrangian multipliers are available the right-hand-side vector $\bar{m}^{\text{eff}}$ for the transition moment Lagrangian multipliers can be set up and Eq. (25) can be solved for the single-excitation part of $\bar{M}$.

(iv) For the calculation of excited-state first-order properties also the right-hand-side vectors $\bar{n}^{\text{eff}}$ are set up and the single excitation parts of the excited-state Lagrangian multipliers are determined from Eq. (28).

(v) In the next step the different one-particle density matrices needed for the calculation of transition moments ($D^{\eta}(E)$, $D^{\xi}(\bar{M})$, $D^{\xi}(\bar{E})$) and excited-state first-order properties (D^{Λ}, $D^{A}(\bar{E},E)$, $D^{\xi}(\bar{N})$) are computed and stored on disk.

(vi) Finally, the transition moments and first-order properties are evaluated from the density matrices and one-electron integrals.

The evaluation of the vector function, i.e., the residual of the ground-state cluster equations, and the contraction of the effective Jacobian matrix defined in Eq. (13) with a trial vector from the right have been described in detail in Ref. 18. The multiplication of $\mathbf{A}^{\text{eff}}_{\mu_1\nu_1}(\omega)$ with a trial vector from the left—needed for the calculation of the left eigenvectors and for the solution of the response equations for the single-excitation parts of the Lagrangian multipliers $\bar{t}_{\mu_1}$, $\bar{M}_{\mu_1}$, and $\bar{N}_{\nu_1}$—involves similar intermediates and contractions as the multiplication with a vector from the right. Thus similar algorithms can be used to evaluate these contractions and we will therefore not discuss them here further.

As can be seen from Table I and Eqs. (34), (38), and (41) the evaluation of the effective right-hand-side vectors for the different Lagrangian multiplier vectors involves similar contractions as needed for the vector function and the transformation of trial vectors with the effective Jacobian. The individual contributions to these vectors can thus again be computed by similar algorithms as described in Ref. 18. The calculation of the vectors $\bar{n}^{\text{eff}}$ and $\bar{m}^{\text{eff}}$ can be summarized as follows:

(i) The double-excitation part of the "left" vector L^{cd}_{kl}, which for $\bar{m}^{\text{eff}}_{\mu_1}$ contains the ground-state Lagrangian multipliers $\bar{t}_{\mu_2}$ and for $\bar{n}^{\text{eff}}_{\mu_1}$ the left eigenvector $\bar{E}_{\mu_2}$, is calculated on-the-fly in a batched loop over two occupied indices and immediately contracted with the three-index ERI's $\hat{B}^Q_{dl}$ to a three-index intermediate $\check{Y}^{0,Q}_{ck}=\Sigma_{ld}L^{cd}_{kl}\hat{B}^Q_{dl}$ which is stored on disk.

(ii) Then a similar intermediate—$\bar{Y}^Q_{ck}=\Sigma_{ld}R^{cd}_{kl}\hat{B}^Q_{ld}$—and $\bar{C}_{ck}=\Sigma_{ld}R^{cd}_{kl}L_{dl}$ are calculated from the double-excitation part of the "right" vector R^{cd}_{kl}, which for both $\bar{m}^{\text{eff}}_{\mu_1}$ and $\bar{n}^{\text{eff}}_{\mu_1}$ is the right eigenvector.

(iii) From $\bar{Y}^Q_{ck}$ and the response Fock matrix $\bar{F}_{pq}$ the intermediates $\bar{E}_{ji}$ and $\bar{E}_{ab}$, defined in Table I, are constructed and used to calculate the contribution σ^0_{ai} of the result vectors.

(iv) In the next step the double-excitation part of the left vector is recalculated once again to construct a Y intermediate from L^{cd}_{kl} and the integrals $\bar{B}^Q_{dl}$. Then the doubles vector F^{cd}_{kl} is constructed and contracted on-the-fly with $\hat{B}^Q_{ld}$ to an-

Downloaded 02 Oct 2002 to 141.52.232.84. Redistribution subject to AIP license or copyright, see http://ojps.aip.org/jcpo/jcpcr.jsp

other Y intermediate which is added to the previously calculated one, resulting in $\check{Y}^{1,Q}_{ck}=\Sigma_{ld}L^{cd}_{kl}\overline{B}^{Q}_{dl}+\Sigma_{ld}F^{cd}_{kl}\hat{B}^{Q}_{ld}$.

(v) The $\check{Y}^0$ and $\check{Y}^1$ are contracted with precomputed integrals $\overline{B}^{Q}_{ik}$ and $\hat{B}^{Q}_{ij}$, giving the σ^{H}_{ai} contribution to the result vectors.

(vi) The σ^{G}_{ai} contribution is combined with σ^{J}_{ai} and calculated from the intermediates $\check{Y}^0$ and $\check{Y}^1$ and different three-index ERI's by a similar algorithm as described in Ref. 18 for the corresponding contribution to the vector function.

(vii) The last contribution σ^{I}_{ai} is calculated from the intermediate $\overline{C}_{ck}$ and the integrals $\hat{B}^{Q}_{ia}$ using the scheme described in Ref. 18 for the Fock matrices $\hat{F}_{ia}$ and $\overline{F}_{ia}$.

The memory requirements for the calculation of the vectors $\overline{m}^{\text{eff}}$ and $\overline{n}^{\text{eff}}$ are about the same as for the ground-state vector function and the transformations with the Jacobian $\mathbf{A}^{\text{eff}}_{\mu_1\nu_1}$, although the disk-space requirements are somewhat larger since more intermediates need to be stored on disk. However, the scaling of the required resources CPU time, memory, and disk space with the system size, i.e., with the number of electrons n and the number of basis functions N, is the same as for ground-state calculations: CPU time scales as $\mathcal{O}(n^2N^3)$, the required minimum memory as $\mathcal{O}(N^2)$, and the required disk space as $\mathcal{O}(nN^2)$.

The right-hand-side vector η^{eff} needed for the calculation of the ground-state Lagrangian multipliers $\overline{t}$ can be obtained as simplification of the vectors $\overline{m}^{\text{eff}}$ and $\overline{n}^{\text{eff}}$: The pure single-excitation contribution $\eta^{(0)}_{ai}$ is twice the intermediate $\hat{F}_{ia}$. The remaining two contributions can be written as $\Sigma_{Qd}\check{Y}^{Q}_{di}\hat{B}^{Q}_{da}$ and $\Sigma_{Ql}\check{Y}^{Q}_{al}\hat{B}^{Q}_{il}$ with $\check{Y}^{Q}_{ck}=\Sigma_{ld}\eta^{cd}_{kl}\hat{B}^{Q}_{dl}$ and can thus be evaluated using the same algorithms as for the σ^{G}_{ai} and σ^{H}_{ai} contributions to $\overline{m}^{\text{eff}}$ and $\overline{n}^{\text{eff}}$.

The last computationally expensive task is the calculation of the different one-electron density matrices which require again the recalculation of double-excitation amplitudes and Lagrangian multipliers. For the explicit formulas see Table II. The computationally difficult contributions are the two contractions $\Sigma_{ijc}L^{ac}_{ij}R^{bc}_{ij}$ and $\Sigma_{bck}L^{ab}_{ik}R^{ab}_{jk}$. To keep the minimum memory requirements down at $\mathcal{O}(N^2)$ the contraction $\Sigma_{ijc}L^{ac}_{ij}R^{bc}_{ij}$ is evaluated in a batched loop over the two occupied orbital indices i and j. Within this loop the doubles excitation amplitudes L^{ac}_{ij} and R^{bc}_{ij} are calculated on-the-fly from the corresponding precomputed three-index ERI's and contracted immediately to the final result by a matrix–matrix multiplication with fixed indices i and j. In the same loop the double-excitation amplitudes R^{ab}_{ij} are contracted with the vector L_{ia} to $\Sigma_{bj}L_{bj}[2R^{ab}_{ij}-R^{ab}_{ji}]$. The contractions $\Sigma_{bck}L^{ab}_{ik}R^{ab}_{jk}$ are evaluated using same algorithm but with occupied and virtual orbital indices interchanged. All other contributions are easily calculated from the single-excitation amplitudes and Lagrangian multipliers and the above-mentioned contractions.

IV. ACCURACY OF THE RI APPROXIMATION

The error in the total energy and in molecular properties introduced by the RI approximation has been shown in several investigations[20–22] to have the same behavior as the one-electron basis set error; i.e., it behaves globally consistent without introducing discontinuities in the hypersurface. The RI error can be kept reasonably small by using optimized auxiliary basis sets. An efficient approach for the optimization has been devised in Ref. 21: The auxiliary basis sets are required to minimize the functional

$$\delta^{RI}=\frac{1}{4}\sum_{iajb}\frac{(\langle ab||ij\rangle-\langle ab||ij\rangle^{RI})^2}{\epsilon_a-\epsilon_i+\epsilon_b-\epsilon_j}, \tag{47}$$

for the atoms in their electronic ground state. Here, i, j and a, b denote, respectively, occupied and virtual spin-orbitals and $\langle ab||ij\rangle$ are antisymmetrized two-electron integrals.

For the calculation of excitation energies and ground- and excited-state expectation values the correlation consistent basis sets augmented with diffuse functions aug-cc-pVXZ with $X=D$, T, Q, ... developed by Dunning and co-workers[28–32] are a very valuable tool since they allow a systematic investigation of basis set effects. In a recent communication,[22] optimized auxiliary basis sets for the series of correlation-consistent basis sets cc-pVXZ and aug-cc-pVXZ ($X=D,T,Q$) were presented. With these auxiliary basis sets, the RI error in the MP2 energy was shown to be about two orders of magnitude smaller than the basis set truncation error. The RI error in the MP2 relaxed first-order properties is about one order of magnitude smaller than the basis set error.

For CC2, two questions arise:

(a) Is the choice of MP2-optimized auxiliary basis sets appropriate for CC2, since here also integrals with three occupied or three virtual indices enter?

(b) Is it necessary to extent the auxiliary basis sets with additional functions if the underlying one-electron basis set is augmented with further diffuse functions (e.g., if Rydberg states are examined)?

A. Typical example: C_2H_4

As a first illustrative example, we study the basis set convergence and the RI error of vertical excitation energies ΔE_v and the isotropic second moment of the electron difference density $\Delta\alpha=1/3(\langle r^2\rangle-\langle r^2\rangle_0)$ of the two lowest $^1B_{1u}$ states of ethene (lying in the xy plane). The first state has largely valence character; the second one is a diffuse Rydberg state. Calculations were carried out at the RI-MP2/TZVPP (Ref. 33) optimized geometry. The frozen core approximation was used throughout. The influence of diffuse functions was tested employing the series x-aug-cc-pVDZ ($x=s,d,t,q$); the basis set convergence was then tested for the sequence d-aug-cc-pVXZ ($X=D,T,Q,5$). The RI-CC2 calculations were carried out using a development version of the RICC2 module of the TURBOMOLE (Ref. 34) package. The conventional CC2 calculations were done with DALTON (Ref. 35). The auxiliary basis sets from Ref. 22 were used. The quintuple ζ calculation was carried out in the RI approximation only, using a specially optimized auxiliary basis set for carbon and hydrogen (available from the authors). The results are depicted in Figs. 1 and 2.

With respect to additional diffuse functions, the valence state converges at the doubly augmented level, while for the Rydberg state at least three sets of diffuse functions are nec-

Downloaded 02 Oct 2002 to 141.52.232.84. Redistribution subject to AIP license or copyright, see http://ojps.aip.org/jcpo/jcpcr.jsp

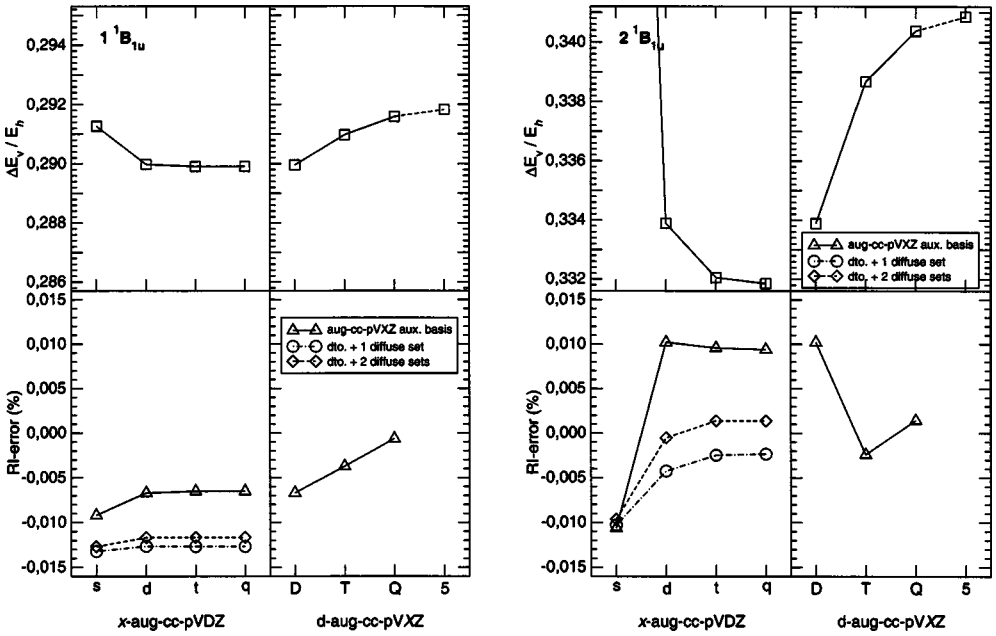


FIG. 1. Basis set convergence and RI error of vertical CC2 excitation energies for ethene $^1B_{1u}$ valence and Rydberg states.

essary in the one-electron basis. The RI error is small, below 0.02% for the excitation energy and 0.4% for $\Delta\alpha$. Additional diffuse *auxiliary* functions improve the result little. However, for the vertical excitation energy of the valence state this is not the case, and for $\Delta\alpha$ of the Rydberg state the improvement is not convincing either.

The necessity of additional diffuse auxiliary functions becomes even more questionable if the basis set convergence with respect to basis functions with higher angular momenta is taken into account. While saturation with diffuse functions is achieved soon, the convergence of the cardinal expansion (where the cardinal number X refers to the respective basis set in the series aug-cc-pVXZ) is known to be very slow.[36,37] The limit is only accessible using explicitly correlated methods[38–40] or extrapolation schemes.[37,41] Relative to this kind of basis-set-induced uncertainty, the RI error is clearly negligible. Furthermore, we find that with the auxiliary basis sets aug-cc-pVTZ and aug-cc-pVQZ the RI error is more diminished than by additional diffuse sets of functions at the double-ζ level.

The explanation for this is that convergence to the basis set limit is for both the one-electron and the auxiliary basis, only obtained in the cardinal expansion and not by just augmenting with diffuse functions. At the aug-cc-pVXZ level for the auxiliary basis set the dominating error apparently stems from the incompleteness in the valence region and not from the incompleteness with respect to diffuse functions, irrespective of the augmentation level of the one-electron basis.

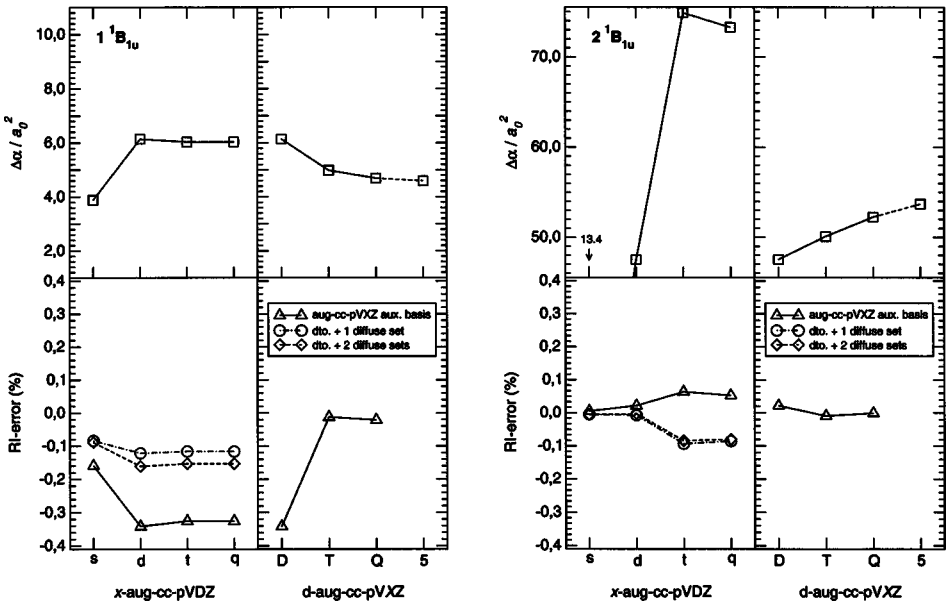


FIG. 2. Basis set convergence and RI error of the second moment of the CC2 difference density for ethene $^1B_{1u}$ valence and Rydberg states.

Downloaded 02 Oct 2002 to 141.52.232.84. Redistribution subject to AIP license or copyright, see http://ojps.aip.org/jcpo/jcpcr.jsp

TABLE III. Test set of 29 sample molecules (248 excited states). The number of states considered for each molecule is given in parentheses.

Row 1	Row 2	Row 3
H_2 (5), HeH^+ (2), BH_2F (10), BH_2NH_2 (10), C_2H_4 (12), CH_2F^+ (9), CH_2NH (8), CH_2O (11), CO_2 (5), N_2 (5), H_2O (9), NeH^+ (4)	AlH_2NH_2 (12), OAlF (10), SiH_2 (12), SiH_2O (12), H_2POH (10), HCP (10), SF_2 (11), H_2S_2 (12), CCl_2 (12), ClF (6), ArH^+ (4)	GaH_3 (7), GeH_2 (8), AsH_2Cl (10), SeH_2 (10), BBr (9), KrH^+ (4)

B. Investigation of the RI error

For a single molecule, this result may be fortuitous. Therefore, we have set up a test set of 29 small molecules and 248 excited states, respectively, as displayed in Table III. As in Ref. 22, the set is divided into first-row, second-row, and third-row compounds. Only a few representatives for third-row element compounds were chosen due to the problem of excluding the semivalence *d* shell from the correlation treatment: This is not possible if the *d* shell becomes near degenerate with low-lying valence shells of other atoms in the molecule.[31] However, the correlation-consistent basis sets are currently not designed for correlation of the *d* electrons; cf. Refs. 31 and 22. Thus, mainly only hydrides of these elements were chosen and the *d* shell was kept frozen. The geometries of the molecules have been optimized at the RI-MP2/TZVPP (Ref. 33) level. As in the preceding section, the RI-CC2 calculations employed a development version of the RICC2 module of the TURBOMOLE (Ref. 34) package while the conventional CC2 calculations were done with DALTON (Ref. 35). We used again the correlation-consistent basis sets aug-cc-pVXZ and n-aug-cc-pVDZ ($X=D,T,Q$; $n=s,d,t$) of Dunning and co-workers in connection with the recently published auxiliary basis sets. For Al-Ar the aug-cc-pV($X+d$)Z basis sets were used throughout.

In Table IV, the relative basis set error and the relative RI error in the ground-state MP2 and CC2 correlation energies are displayed. Both energies are normalized with respect to the basis set limit, which has been estimated by two-point extrapolation of the aug-cc-pVTZ and aug-cc-pVQZ results.[37] It is clearly demonstrated that the same accuracy of the RI approximation is obtained for both RI-MP2 and RI-CC2 correlation energies. This is the expected result, since the dominant contributions to the CC2 energy originate from MP2-like terms. The average error, the standard deviation, the average absolute error, and the maximum error are very small (maximum error below 0.15%) and the latter three errors also decrease significantly for the larger aug-cc-pVTZ and aug-cc-pVQZ auxiliary basis sets. This has to be contrasted with the mean basis set error which is 30%, 10%, and 4% at the double-, triple-, and quadruple-ζ levels, respectively. These findings are in perfect agreement with those of Ref. 22.

In order to characterize the RI error for excited states, we examined vertical excitation energies ΔE_v, the oscillator strengths (velocity gauge) f^v, the isotropic second moment of the difference density $\Delta\alpha$, and the change in the dipole moment $\Delta\mu$. The results are listed in Tables V–IX.

The RI error in the vertical excitation energies is well below 0.01 eV. The largest errors found in our test set are 5 meV (the largest relative error is 0.12%). As for the ground-state correlation energies, no significant difference is found comparing results for the first-, second-, and third-row compounds. The mean absolute error, being a measure for the typical RI error to be expected in calculations, decreases as 1.3, 0.4, and 0.2 meV for double-, triple-, and quadruple-ζ calculations. Similarly the mean error and the standard deviation become smaller. No marked differences in the error statistics for the doubly and triply augmented basis sets is found although for these the same fitting basis is used. This confirms the findings for the ethene example above. The relatively large maximum error obtained in the aug-cc-pVQZ basis originates from the $1\,^1\Delta_u$ state of N_2 (2.1 meV). This state and the $1\,^1\Sigma_u^-$ state of N_2 (deviation 1.5 meV) are, however, the only cases with errors larger than 0.5 meV for the aug-cc-pVQZ basis in our test set.

The oscillator strength was examined in the velocity gauge; results in the length gauge are essentially the same.

TABLE IV. Relative basis set and RI error in MP2 and CC2 ground-state correlation energies. The basis set limit is extrapolated from the triple- and quadruple-ζ results. The errors are defined as $\Delta=(E_X^{\mathrm{corr}}-E_{\mathrm{lim}}^{\mathrm{corr}})/E_{\mathrm{lim}}^{\mathrm{corr}}\times 100\%$ and $\Delta=(E_{X,RI}^{\mathrm{corr}}-E_X^{\mathrm{corr}})/E_{\mathrm{lim}}^{\mathrm{corr}}\times 100\%$ respectively.

	aug-cc-pVDZ[a]		aug-cc-pVTZ[a]		aug-cc-pVQZ[a]	
	Basis	RI	Basis	RI	Basis	RI
MP2						
$\langle\Delta\rangle$	27.187	0.007	10.417	0.008	4.395	0.006
σ_Δ	3.817	0.032	1.739	0.009	0.734	0.004
$\langle\lvert\Delta\rvert\rangle$	27.187	0.017	10.417	0.008	4.395	0.006
max$\lvert\Delta\rvert$	37.129	0.157	14.551	0.042	6.139	0.024
CC2						
$\langle\Delta\rangle$	26.979	0.005	10.303	0.007	4.347	0.006
σ_Δ	3.769	0.032	1.704	0.009	0.719	0.004
$\langle\lvert\Delta\rvert\rangle$	26.979	0.017	10.303	0.007	4.347	0.006
max$\lvert\Delta\rvert$	37.015	0.157	14.524	0.043	6.127	0.024

[a]For Al-Ar the respective x-aug-cc-pV($X+d$)Z basis sets were used.

Downloaded 02 Oct 2002 to 141.52.232.84. Redistribution subject to AIP license or copyright, see http://ojps.aip.org/jcpo/jcpcr.jsp

TABLE V. Absolute RI errors (meV) in vertical excitation energies. The auxiliary basis sets optimized for aug-cc-pVXZ have been used (no further diffuse functions were added).

	aug-cc-pVDZ[a]	d-aug-cc-pVDZ[a]	t-aug-cc-pVDZ[a]	aug-cc-pVTZ[a]	aug-cc-pVQZ[a]
All ($n=248$)					
$\langle\Delta^{\mathrm{RI}}\rangle$	−1.13	−1.02	−1.03	−0.37	−0.16
$\sigma_{\Delta^{\mathrm{RI}}}$	1.09	1.08	1.09	0.34	0.20
$\langle\lvert\Delta^{\mathrm{RI}}\rvert\rangle$	1.23	1.20	1.20	0.39	0.17
$\max\lvert\Delta^{\mathrm{RI}}\rvert$	5.14	5.00	5.03	2.02	2.10

[a]For Al-Ar the respective x-aug-cc-pV($X+d$)Z basis sets were used.

The results are summarized in Table VI. For oscillator strengths above 0.001 we find mean absolute errors of 0.28%–0.36%, 0.07%, or 0.03% for double, triple, and quadruple ζ, respectively. The spread is somewhat larger than for excitation energies and we find maximum errors of 3.8%–4.7%, 0.8%, and 0.6%. Again, no significant change of the RI error for the doubly and triply augmented basis sets of double ζ is observed. We note that the errors for second- and third-row elements are a bit larger, especially for the double-ζ calculations.

The oscillator strengths below 0.001 are collected in a separate statistic. We find absolute RI errors of the order 1×10^{-4} (double ζ) to 1×10^{-5} (quadruple ζ). Relative errors are eventually larger than for the stronger transitions discussed in the preceeding paragraph. However, for near-zero values the relative error is meaningless in practice.

For $\Delta\alpha$ the results were subdivided in a similar fashion. We chose a value of 1 a.u., which for the small molecules in the current test set also constitutes a weak criterion whether a valence state or a mixed or Rydberg state is present.

In both cases ($\Delta\alpha<1$ and $\Delta\alpha>1$) we find the RI error to increase with additional diffuse functions in the one-electron basis sets (cf. Table VII). For aug-cc-pVTZ and aug-cc-pVQZ it becomes smaller again. We redid the calculations in the t-aug-cc-pVDZ basis using other auxiliary basis sets (Table VIII). First, we tested an aug-cc-pVDZ fitting basis augmented with a set of diffuse functions, which were extrapolated for each l quantum number from the lowest exponents. The results for $\Delta\alpha>1$ are improved by roughly a factor of 1.5, whereas the cases with small $\Delta\alpha$ do not change significantly. However, if instead the aug-cc-pVTZ auxiliary basis set is used (without adding further diffuse functions), results for both regimes of $\Delta\alpha$ are improved by nearly one order of magnitude. This demonstrates clearly that the most important source of the RI error is not a lack of diffuse functions; the problem is rather to correctly fit the density in the valence region of the ionic core in Rydberg states.

A similar picture is encountered for the change of the dipole moment upon excitation. The mean absolute error is 0.1%–0.2%, 0.03%, and 0.02% for the double-, triple-, and quadruple-ζ calculations, respectively. For small changes in the dipole moment ($\Delta\mu<0.5$ a.u.), maximum errors are of the order 2×10^{-2} a.u. for x-aug-cc-pVDZ, and 3×10^{-3} a.u. for aug-cc-pVTZ and aug-cc-pVQZ. The error again increases, if diffuse functions are added. Similar as described above for $\Delta\alpha$ the main source of error is found to be the fitting of the valence region.

C. RI error versus basis set convergence

For excited-state energies, transition moments, and properties, so far no extrapolation scheme has been established and thoroughly tested. Therefore we take the aug-cc-pVQZ result as the best estimate. The basis set error in the sense of convergence with respect to the ζ level is only meaningful if the result is converged with respect to saturation with diffuse

TABLE VI. RI errors in the oscillator strength (velocity gauge). The auxiliary basis sets optimized for aug-cc-pVXZ have been used (no further diffuse functions were added).

Absolute RI error (ppm) for very weak transitions ($f^v<0.001$)					
	aug-cc-pVDZ[a] $n=17$	d-aug-cc-pVDZ[a] $n=18$	t-aug-cc-pVDZ[a] $n=24$	aug-cc-pVTZ[a] $n=18$	aug-cc-pVQZ[a] $n=21$
$\langle\Delta^{\mathrm{RI}}\rangle$	−2.9	−3.4	−3.4	−0.1	0.4
$\sigma_{\Delta^{\mathrm{RI}}}$	12.3	15.0	13.5	2.5	1.3
$\langle\lvert\Delta^{\mathrm{RI}}\rvert\rangle$	8.9	10.4	9.3	1.8	0.9
$\max\lvert\Delta^{\mathrm{RI}}\rvert$	29.1	37.5	38.1	5.8	4.9
Relative RI error (%) for transitions with $f^v>0.001$					
	aug-cc-pVDZ[a] $n=159$	d-aug-cc-pVDZ[a] $n=158$	t-aug-cc-pVDZ[a] $n=152$	aug-cc-pVTZ[a] $n=157$	aug-cc-pVQZ[a] $n=155$
$\langle\Delta^{\mathrm{RI}}\rangle$	−0.05	−0.01	0.00	−0.01	−0.01
$\sigma_{\Delta^{\mathrm{RI}}}$	0.59	0.69	0.76	0.13	0.07
$\langle\lvert\Delta^{\mathrm{RI}}\rvert\rangle$	0.28	0.34	0.36	0.07	0.03
$\max\lvert\Delta^{\mathrm{RI}}\rvert$	3.73	4.59	4.68	0.76	0.57

[a]For Al-Ar the respective x-aug-cc-pV($X+d$)Z basis sets were used.

Downloaded 02 Oct 2002 to 141.52.232.84. Redistribution subject to AIP license or copyright, see http://ojps.aip.org/jcpo/jcpcr.jsp

TABLE VII. RI errors in the change of the second moment of charge $\Delta\alpha$. The auxiliary basis sets optimized for aug-cc-pVXZ have been used (no further diffuse functions were added).

	aug-cc-pVDZ[a] $n=31$	d-aug-cc-p$V D$Z[a] $n=28$	t-aug-cc-pVDZ[a] $n=26$	aug-cc-pVTZ[a] $n=33$	aug-cc-pVQZ[a] $n=34$
Absolute RI error (10^{-3} a.u.) for transitions with $\Delta\alpha<1$ a.u.					
$\langle\Delta^{RI}\rangle$	−0.28	−0.73	−0.50	−0.10	−0.02
$\sigma_{\Delta^{RI}}$	1.12	1.84	1.59	0.13	0.05
$\langle\lvert\Delta^{RI}\rvert\rangle$	0.69	0.90	0.69	0.12	0.04
$\max\lvert\Delta^{RI}\rvert$	4.60	7.94	8.13	0.54	0.19
Relative RI error (%) for transitions with $\Delta\alpha>1$ a.u.					
	aug-cc-pVDZ[a] $n=217$	d-aug-cc-pVDZ[a] $n=220$	t-aug-cc-pVDZ[a] $n=222$	aug-cc-pVTZ[a] $n=215$	aug-cc-pVQZ[a] $n=214$
$\langle\Delta^{RI}\rangle$	−0.03	−0.03	−0.05	−0.01	−0.01
$\sigma_{\Delta^{RI}}$	0.10	0.15	0.15	0.05	0.03
$\langle\lvert\Delta^{RI}\rvert\rangle$	0.06	0.09	0.08	0.02	0.01
$\max\lvert\Delta^{RI}\rvert$	0.61	0.96	1.00	0.56	0.31

[a]For Al-Ar the respective x-aug-cc-pV$(X+d)$Z basis sets were used.

functions. Hence, only those states were included which do not differ more than 5% for the respective property when going from aug-cc-pVDZ to d-aug-cc-pVDZ. The vertical excitation energies were in addition required to differ by less than 0.2 eV between the aug-cc-pVDZ and the aug-cc-pVTZ basis. Thus, the test set employed in this section is restricted to valence states. The results are summarized in Table X.

The most important finding is that in all cases the RI error is nearly two orders of magnitude smaller than the corresponding basis set error. For instance excitation energies have a mean absolute deviation from the aug-cc-pVQZ result of approximately 0.08 eV at the double-ζ level and 0.02 eV at the triple-ζ level. The associated mean absolute RI error is 1.1 meV at the double-ζ level and 0.4 meV at the triple-ζ level. It is interesting to note that the mean basis set error $\langle\Delta\rangle$ is negative, indicating that typically the excitation energies will increase when a larger basis set is employed. Very similar results are obtained for oscillator strengths and excited state properties.

Strictly, this has only been established for valence states in this section. For diffuse states the d-aug-pVXZ or even t-aug-pVXZ series must be employed which is too time-consuming for a conventional CC2 implementation. However, no serious deviations from our present conclusions are expected from such a study. Concerning the one-electron basis set convergence it was found in previous studies[26,42–44] that excitation energies of Rydberg states always increase when the basis sets are enlarged.

D. Larger molecules: Benzene

Rydberg states of somewhat larger molecules like benzene are studied using special Rydberg-basis functions which are located at the center of charge (in the case of benzene identical with the center of mass c.m.). In the course of such a study,[26] the question arose, whether and how to consider these in the fitting basis.

The basis set considered here is aug-cc-pVDZ+c.m.2, where c.m.2 is an uncontracted $2s2p2d$ set with exponents 0.01 and 0.0033 for each shell. Larger basis sets were too time consuming for the conventional CC2 calculations. As fitting basis sets the aug-cc-pVDZ optimized basis was considered (a) without further augmentation, (b) with additional diffuse auxiliary basis functions obtained by extrapolation, and (c) with additional diffuse auxiliary basis functions at the center of mass ($4s4p4d4f$; exponents 0.02, 0.01, 0.0066, 0,0033). For comparison also the aug-cc-pVTZ optimized fitting basis was included. The ''test set'' here consists of the 19 lowest excited states.

From the results displayed in Table XI it is evident that no diffuse auxiliary functions are necessary. Neither the atom centered diffuse functions nor the center-of-mass functions change the results significantly. No qualitative difference in the results for the four valence states, which are included in the test set, and the Rydberg states was found. The RI error is

TABLE VIII. Influence of different auxiliary basis sets on the change of the second moment of charge $\Delta\alpha$ for t-aug-cc-pVDZ basis sets. The auxiliary basis sets optimized for aug-cc-pVDZ and aug-cc-pVTZ have been used: the set of diffuse functions used in the middle column has been obtained by extrapolation from the two most diffuse functions of each l quantum number.

Basis Auxbasis	t-aug-cc-pVDZ[a] aug-cc-pVDZ	t-aug-cc-pVDZ[a] aug-cc-pVDZ+diffuse	t-aug-cc-pVDZ[a] aug-cc-pVTZ
Absolute RI error (10^{-3} a.u.) for transitions with $\Delta\alpha<1$ a.u.			
$\langle\Delta^{RI}\rangle$	−0.50	−0.57	−0.01
$\sigma_{\Delta^{RI}}$	1.59	1.77	0.06
$\langle\lvert\Delta^{RI}\rvert\rangle$	0.69	0.73	0.04
$\max\lvert\Delta^{RI}\rvert$	8.13	9.22	0.26
Relative RI error (%) for transitions with $\Delta\alpha>1$ a.u.			
Basis Auxbasis	t-aug-cc-pVDZ[a] aug-cc-pVDZ	t-aug-cc-pVDZ[a] aug-cc-pVDZ+diffuse	t-aug-cc-pVDZ[a] aug-cc-pVTZ
$\langle\Delta^{RI}\rangle$	−0.05	−0.05	0.00
$\sigma_{\Delta^{RI}}$	0.15	0.10	0.03
$\langle\lvert\Delta^{RI}\rvert\rangle$	0.08	0.06	0.02
$\max\lvert\Delta^{RI}\rvert$	1.00	0.70	0.16

[a]For Al-Ar the respective x-aug-cc-pV$(X+d)$Z basis sets were used.

Downloaded 02 Oct 2002 to 141.52.232.84. Redistribution subject to AIP license or copyright, see http://ojps.aip.org/jcpo/jcpcr.jsp

TABLE IX. RI errors in the change of the dipole moment $\Delta\mu$. The auxiliary basis sets optimized for aug-cc-$pVXZ$ have been used (no further diffuse functions were added).

Absolute RI error (10^{-3} a.u.) for transitions with $\Delta\mu<0.5$ a.u.					
$\Delta\mu<0.5$ a.u.	aug-cc-$pVDZ$[a] $n=60$	d-aug-cc-$pVDZ$[a] $n=53$	t-aug-cc-$pVDZ$[a] $n=54$	aug-cc-$pVTZ$[a] $n=61$	aug-cc-$pVQZ$[a] $n=61$
$\langle\Delta^{RI}\rangle$	−0.27	−0.90	1.09	−0.04	−0.11
$\sigma_{\Delta^{RI}}$	3.18	5.27	5.63	0.66	0.54
$\langle\lvert\Delta^{RI}\rvert\rangle$	1.56	2.94	3.15	0.40	0.21
$\max\lvert\Delta^{RI}\rvert$	17.82	21.23	23.86	2.97	3.85
Relative RI error (%) for transitions with $\Delta\mu>0.5$ a.u.					
	aug-cc-$pVDZ$[a] $n=159$	d-aug-cc-$pVDZ$[a] $n=166$	t-aug-cc-$pVDZ$[a] $n=165$	aug-cc-$pVTZ$[a] $n=158$	aug-cc-$pVQZ$[a] $n=158$
$\langle\Delta^{RI}\rangle$	−0.01	−0.01	−0.03	0.01	0.01
$\sigma_{\Delta^{RI}}$	0.12	0.30	0.37	0.07	0.05
$\langle\lvert\Delta^{RI}\rvert\rangle$	0.07	0.18	0.22	0.03	0.02
$\max\lvert\Delta^{RI}\rvert$	0.86	1.68	1.63	0.76	0.48

[a]For Al-Ar the respective x-aug-cc-$pV(X+d)Z$ basis sets were used.

within the range expected from the results of the previous sections and is solely determined by the quality of the fitting basis at the atoms. The latter is demonstrated by applying the larger aug-cc-$pVTZ$ auxiliary basis which now significantly decreases the errors. However, it also increases the computation time by nearly 40% without significantly improving the overall accuracy which is limited by the one-electron basis set error and the correlation error inherent to the CC2 method.

This result is in line with the findings for Rydberg states in the previous sections.

V. EFFICIENCY OF THE T_2-DIRECT RI-CC2 APPROACH

The T_2-direct code has been developed with the scope of large-scale calculations. As discussed in Ref. 26 the conventional approach, which stores N^4 intermediates, is restricted

TABLE X. Comparison of RI and basis set errors for vertical excitation energies (meV), oscillator strengths (velocity gauge, 10^{-3}), change in the second moments of charge (10^{-3} a.u.), and change in the dipole moments (10^{-3} a.u.). The errors for each observable O are defined as $\Delta^{basis}=(O_X-O_Q)$ and $\Delta^{RI}=(O_{X,RI}-O_X)$, respectively.

	aug-cc-$pVDZ$[a]		aug-cc-$pVTZ$[a]		aug-cc-$pVQZ$[a]
	Basis	RI	Basis	RI	RI
ΔE_{vert} ($n=132$)					
$\langle\Delta\rangle$	−36.57	−1.03	−16.59	−0.34	−0.14
σ_Δ	89.17	1.07	24.54	0.30	0.11
$\langle\lvert\Delta\rvert\rangle$	81.30	1.11	23.18	0.36	0.15
$\max\lvert\Delta\rvert$	223.09	4.92	112.67	2.02	0.55
f^v ($n=32$)					
$\langle\Delta\rangle$	−0.80	−0.03	−0.22	−0.01	0.00
σ_Δ	4.55	0.12	1.07	0.03	0.01
$\langle\lvert\Delta\rvert\rangle$	3.53	0.05	0.80	0.02	0.01
$\max\lvert\Delta\rvert$	12.82	0.67	2.99	0.17	0.03
$\Delta\alpha$ ($n=56$)					
$\langle\Delta\rangle$	227.15	−1.06	41.55	−0.14	−0.13
σ_Δ	493.98	2.20	285.06	0.95	0.26
$\langle\lvert\Delta\rvert\rangle$	297.37	1.62	107.56	0.41	0.18
$\max\lvert\Delta\rvert$	1962.67	9.66	1848.31	6.67	1.23
$\Delta\mu$ ($n=57$)					
$\langle\Delta\rangle$	21.85	−0.12	5.73	−0.05	0.00
σ_Δ	136.33	0.64	51.44	0.25	0.12
$\langle\lvert\Delta\rvert\rangle$	83.27	0.46	21.90	0.15	0.07
$\max\lvert\Delta\rvert$	551.21	2.17	301.19	1.12	0.63

[a]For Al-Ar the respective x-aug-cc-$pV(X+d)Z$ basis sets were used.

Downloaded 02 Oct 2002 to 141.52.232.84. Redistribution subject to AIP license or copyright, see http://ojps.aip.org/jcpo/jcpcr.jsp

TABLE XI. Relative RI error (%) of excitation energy, change of electronic second moment ($\Delta\alpha$) and oscillator strength (velocity gauge) for 19 excited states of benzene. The aug-cc-pVDZ basis set augmented with a set of center-of-mass functions and the geometry of Ref. 45 was used in connection with different RI basis sets (see text).

Auxiliary basis	aug-cc-pVDZ	+extrapolated	+c.m.(4,4,4,4)	aug-cc-pVTZ
ΔE ($n=19$)				
$\langle\Delta\rangle$	0.0030	0.0059	0.0038	0.0010
σ_Δ	0.0039	0.0049	0.0042	0.0008
$\langle\|\Delta\|\rangle$	0.0045	0.0073	0.0054	0.0010
max(Δ)	0.0083	0.0101	0.0085	0.0029
$\Delta\alpha$ ($n=19$)				
$\langle\Delta\rangle$	0.002	−0.014	−0.004	−0.008
σ_Δ	0.108	0.107	0.098	0.012
$\langle\|\Delta\|\rangle$	0.051	0.053	0.050	0.010
max(Δ)	0.379	0.363	0.332	0.046
f^v($n=4$)				
$\langle\Delta\rangle$	−0.012	0.014	−0.028	0.006
σ_Δ	0.347	0.365	0.332	0.036
$\langle\|\Delta\|\rangle$	0.249	0.243	0.249	0.025
max(Δ)	0.474	0.514	0.443	0.054

to calculations with below approximately 4×10^8 double-excitation amplitudes (requiring 3 GB of disk space for each doubles intermediate), e.g., $\approx$40 occupied orbitals and $\approx$500 basis functions in C_1 symmetry. It is, however, interesting to note that even for small molecules as employed in the above test set, the RI approximation makes the code very efficient.

In Table XII the timings of SF_2 are presented. All these timings were obtained on standard Athlon 1.2GHz PCs with 750 MB RAM and 25 GB mass storage.

For the aug-cc-pVDZ basis set, the RI code is only slightly faster. Augmentation with further diffuse functions increases the computation times of RI-CC2 only slowly (by a factor of 2), while the timings of the conventional code increase by a factor of 8. This reflects the fact that the size of the auxiliary basis set stays constant, which leads to a lower scaling of the time determining steps.

At the triple-ζ level the RI calculation runs 5 times faster than its conventional counterpart. The CPU/wall ratio of conventional nondirect calculations begins to drop significantly due to the limited I/O rate of the PC system employed; for other triple-ζ examples of the test set with more than 150 basis functions the observed ratio goes down to 0.5.

In the quadruple-ζ basis, the conventional CC2 calculations were all run either in the integral-direct mode[24] or on workstations with fast I/O capacities. The RI code still runs efficiently on the standard PC's. For SF_2 it is over 50 times faster than the conventional calculation. The largest calculation in the test set was AlH_2NH_2 (353 basis function in C_{2v} symmetry), which took only 340 min for 12 states.

These observations confirm the efficiency of the current CC2 approach. As already stated in previous studies on RI-MP2,[21,22] the RI approximation becomes increasingly efficient for large basis sets, as the most expensive step, Eq. (11), scales with $O^2V^2N_x$. Large-scale applications of the RI-CC2 approach for transition moments and first-order properties of excited states have already been reported in two previous communications where the excited states of benzene[26] and trans-azobenzene[27] were studied employing up to 828 and 874 basis functions, respectively.

VI. CONCLUSIONS

We have presented a partitioned, T_2-direct formulation of the CC2 response equations, which allows us to calculate transition moments and ground- and excited-state first-order properties without the need of storing any N^4 intermediates either in memory or on disk. In connection with the RI approximation for the electron repulsion integrals this leads to a very efficient implementation, which extends the applicability of the CC2 method significantly. Already for relatively small molecules the performance is much improved. Unlike for the conventional implementation in DALTON,[35] all calculations for the present investigation could be run with low computational requirements, especially concerning the I/O.

The accuracy of the RI approximation and convergence with respect to the one-electron basis set has been studied for the CC2 ground state and excitation energies, transition moments, and first-order properties of excited states. The test set employed in the present investigation, which consists of 29 molecules and 248 excited states, does not reveal any serious problems with auxiliary basis sets optimized for MP2 correlation energies, at least for the correlation-consistent basis sets used in the present study. We find errors of typically 1 meV and below for excitation energies, with relative errors below 0.1%. Oscillator strengths exhibit RI errors of at most 5% for the x-aug-cc-pVDZ basis sets and below 1% for aug-cc-pVTZ and aug-cc-pVQZ. For excited-state first-

TABLE XII. Timings for the SF_2 molecule obtained with RI-CC2 and a conventional CC2 implementation (DALTON). The elapsed wall time and CPU time for the coupled-cluster part (ground state and 11 excited states including transition moments and first-order properties) are given. N is the number of basis functions. All examples were run on an Athlon 1.2 GHz system with 750 MHz memory and 25 GB mass storage.

		t_{RICC2}		t_{CC2}	
	N	Wall	CPU	Wall	CPU
aug-cc-pVDZ[a]	78	13.2	13.2	21.3	20.9
d-aug-cc-pVDZ[a]	105	15.5	15.5	67.3	66.6
t-aug-cc-pVDZ[a]	132	22.8	22.8	168.1	166.0
aug-cc-pVTZ[a]	147	44.4	44.4	221.3	211.6
aug-cc-pVQZ[a]	249	189.9	189.7	12984.8[b]	10692.6[b]

[a]For sulfur the respective x-aug-cc-pV($X+d$)Z basis set was used.
[b]Integral-direct run.

Downloaded 02 Oct 2002 to 141.52.232.84. Redistribution subject to AIP license or copyright, see http://ojps.aip.org/jcpo/jcpcr.jsp

order properties the relative RI errors are at most about 1%, unless the respective transition moment or differential property is very small. The aug-cc-$pVXZ$ auxiliary basis sets are found to be sufficient even for the description of diffuse states. Additional diffuse auxiliary functions are only of minor importance. For the investigated energies and properties the RI error is found to be between one and two orders of magnitude smaller than the corresponding one-electron basis set errors. Thus, this error does not diminish the accuracy of the calculations; nor does it constitute a problem for basis set extrapolation schemes.

For the convergence with respect to the one-electron basis set, we found for the 132 valence states in the present test set that excitation energies have at the aug-cc-$pVDZ$ level mean absolute basis set errors of about 0.08 eV and at the aug-cc-$pVTZ$ level of 0.02 eV, with the tendency that the excitation energies are underestimated in the smaller basis sets; i.e., $\langle\Delta\rangle$ is found to be negative. These findings are in agreement with what has been observed before in studies on some individual molecules.[42–44,26] For oscillator strengths mean absolute basis set errors of about 3.5×10^{-3} (aug-cc-$pVDZ$) and 0.8×10^{-3} (aug-cc-$pVTZ$) are found. Thus, the error decreases from the double- to triple-ζ level by a factor of about 4, which is almost the same factor as for the excitation energies. Similar results are found for the change of the second moment of charge and of the dipole moment upon excitation.

The implementation presented here has already been employed in investigations of the excited states of benzene and of trans-azobenzene. Forthcoming publications will report the spectra of free-base porphyrin and helicenes.

ACKNOWLEDGMENTS

This work was supported by the Deutsche Forschungsgemeinschaft, SFB 195 (''Lokalisierung von Elektronen in makroskopischen und mikroskopischen Systemen'') and the Fonds der Chemischen Industrie.

[1] J. Linderberg and Y. Öhrn, *Propagators in Quantum Chemistry* (Academic, London, 1973).
[2] J. Olsen and P. Jørgensen, J. Chem. Phys. **82**, 3235 (1985).
[3] J. Oddershede, Adv. Chem. Phys. **69**, 201 (1967).
[4] J. Olsen and P. Jørgensen, in *Modern Electronic Structure Theory*, edited by D. R. Yarkony (World Scientific, Singapore, 1995), Vol. 2, Chap. 13, pp. 857–990.
[5] O. Christiansen, P. Jørgensen, and C. Hättig, Int. J. Quantum Chem. **68**, 1 (1998).
[6] H. Larsen, P. Jørgensen, J. Olsen, and T. Helgaker, J. Chem. Phys. **113**, 8908 (2000).
[7] F. Furche, J. Chem. Phys. **114**, 5982 (2001).
[8] P. Jørgensen, H. J. A. Jensen, and J. Olsen, J. Chem. Phys. **89**, 3654 (1988).
[9] H. J. Monkhorst, Int. J. Quantum Chem., Quantum Chem. Symp. **11**, 421 (1977).
[10] H. Sekino and R. J. Bartlett, Int. J. Quantum Chem., Quantum Chem. Symp. **18**, 255 (1984).
[11] J. Geertsen, M. Rittby, and R. J. Bartlett, Chem. Phys. Lett. **164**, 57 (1989).
[12] H. Koch and P. Jørgensen, J. Chem. Phys. **93**, 3333 (1990).
[13] H. Koch, O. Christiansen, P. Jørgensen, and J. Olsen, Chem. Phys. Lett. **244**, 75 (1995).
[14] O. Christiansen, H. Koch, P. Jørgensen, and J. Olsen, Chem. Phys. Lett. **256**, 185 (1996).
[15] O. Christiansen, H. Koch, and P. Jørgensen, Chem. Phys. Lett. **243**, 409 (1995).
[16] H. Koch, O. Christiansen, P. Jørgensen, A. S. de Merás, and T. Helgaker, J. Chem. Phys. **106**, 1808 (1997).
[17] O. Christiansen, H. Koch, and P. Jørgensen, J. Chem. Phys. **103**, 7429 (1995).
[18] C. Hättig and F. Weigend, J. Chem. Phys. **113**, 5154 (2000).
[19] O. Vahtras, J. E. Almlöf, and M. W. Feyereisen, Chem. Phys. Lett. **213**, 514 (1993).
[20] F. Weigend and M. Häser, Theor. Chim. Acta **97**, 331 (1997).
[21] F. Weigend, M. Häser, H. Patzelt, and R. Ahlrichs, Chem. Phys. Lett. **294**, 143 (1998).
[22] F. Weigend, A. Köhn, and C. Hättig, J. Chem. Phys. **116**, 3175 (2002).
[23] H. Koch, O. Christiansen, R. Kobayashi, P. Jørgensen, and T. Helgaker, Chem. Phys. Lett. **228**, 233 (1994).
[24] O. Christiansen, A. Halkier, H. Koch, P. Jørgensen, and T. Helgaker, J. Chem. Phys. **108**, 2801 (1998).
[25] C. Hättig, O. Christiansen, and P. Jørgensen, J. Chem. Phys. **108**, 8331 (1998).
[26] C. Hättig, A. Köhn, and K. Hald, J. Chem. Phys. **116**, 5401 (2002).
[27] C. Hättig and K. Hald, Phys. Chem. Chem. Phys. **4**, 2111 (2002).
[28] T. H. Dunning, J. Chem. Phys. **90**, 1007 (1989).
[29] D. E. Woon and T. H. Dunning, J. Chem. Phys. **98**, 1358 (1993).
[30] D. E. Woon and T. H. Dunning, J. Chem. Phys. **100**, 2975 (1994).
[31] A. K. Wilson, D. E. Woon, K. A. Peterson, and T. H. Dunning, J. Chem. Phys. **110**, 7667 (1999).
[32] T. H. Dunning, K. A. Peterson, and A. K. Wilson, J. Chem. Phys. **114**, 9244 (2001).
[33] A. Schäfer, C. Huber, and R. Ahlrichs, J. Chem. Phys. **100**, 5829 (1994).
[34] R. Ahlrichs, M. Bär, M. Häser, H. Horn, and C. Kölmel, Chem. Phys. Lett. **162**, 165 (1989).
[35] T. Helgaker, H. J. A. Jensen, P. Jørgensen *et al.*, DALTON, an electronic structure program, release 1.2, 2001.
[36] A. Halkier, T. Helgaker, P. Jørgensen, W. Klopper, H. Koch, J. Olsen, and A. K. Wilson, Chem. Phys. Lett. **286**, 243 (1998).
[37] T. Helgaker, W. Klopper, H. Koch, and J. Noga, J. Chem. Phys. **106**, 9639 (1997).
[38] W. Kutzelnigg and W. Klopper, J. Chem. Phys. **94**, 1985 (1991).
[39] W. Klopper and C. C. M. Samson, J. Chem. Phys. **116**, 6397 (2002).
[40] B. J. Persson and P. R. Taylor, J. Chem. Phys. **105**, 5915 (1996).
[41] A. Halkier, W. Klopper, T. Helgaker, and P. Jørgensen, J. Chem. Phys. **111**, 4424 (1999).
[42] O. Christiansen, H. Koch, A. Halkier, P. Jørgensen, T. Helgaker, and A. M. Sanchez de Meras, J. Chem. Phys. **105**, 6921 (1996).
[43] O. Christiansen and P. Jørgensen, J. Am. Chem. Soc. **120**, 3423 (1998).
[44] O. Christiansen, J. Gauss, J. F. Stanton, and P. Jørgensen, J. Chem. Phys. **111**, 525 (1999).
[45] J. Lorentzon, P.-Å. Malmquist, M. Fülscher, and B. O. Roos, Theor. Chim. Acta **91**, 91 (1995).

Downloaded 02 Oct 2002 to 141.52.232.84. Redistribution subject to AIP license or copyright, see http://ojps.aip.org/jcpo/jcpcr.jsp